Macromolecules

Article

Water Swelling Behavior of Poly(ethylene glycol)-Based Polyurethane Networks

Peter T. M. Albers, Leendert G. J. van der Ven, Rolf A. T. M. van Benthem, A. Catarina C. Esteves,* and Gijsbertus de With*
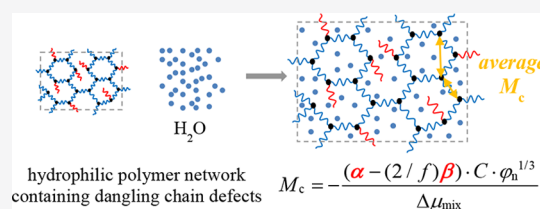
Read Online

ACCESS | Metrics & More | Article Recommendations | Supporting Information

ABSTRACT: Defects in a polymer network complicate an accurate calculation of structural parameters such as the molar mass between cross-links M_c, typically obtained from experimental swelling data. In this paper the formation and structure of poly(ethylene glycol) (PEG)-based polyurethane networks containing PEG-mono methyl ether dangling chains are studied. The phantom network model can describe the swelling behavior of these networks only when a composition-dependent interaction parameter is used and the formation of allophanates is accounted for. A clear transition in the network formation is found at the PEG network precursor molar mass at which entanglements are formed in the melt. Correction factors based on structure calculations using the Miller−Macosko−Vallés probability approach are proposed and validated for an accurate calculation of the M_c of these defect-containing networks. This provides a new approach for studies that requires an accurate estimate of the M_c, only based on experimentally straightforward swelling experiments.

hydrophilic polymer network containing dangling chain defects

$$M_c = -\frac{(\alpha - (2/f)\beta) \cdot C \cdot \varphi_n^{1/3}}{\Delta\mu_{mix}}$$

INTRODUCTION

Cross-linked polymer networks have a widespread use in numerous technical applications of great importance for our daily life, ranging from rubber tires[1,2] to drug release carriers[3,4] and functional coatings,[5,6] among others. The final network properties and morphology depend mainly on the network architecture but also on the chemical nature of the polymer material. For instance, the solvation properties of polymers are utilized for the design of cross-linked networks which swell in the presence of a solvent. A good example of this are hydrogels, which rely on the capacity to absorb a substantial amount of water for the application they are designed for.[3,4,7,8] Although (swollen) polymer networks have been studied for almost a century, a universal and complete theoretical understanding and description of their structure−property relation is still lacking.[9,10] This understanding is severely complicated by the fact that network defects are unavoidably present in all real polymer networks. Such defects are difficult (if not impossible) to detect directly by an experimental approach, and their theoretical description is rather challenging.

The network architecture and structure parameters of a polymer network are of great importance for material (bulk) properties as the network moduli[9,10] and drug-release rate[3,4] as well as surface properties, e.g., antifouling,[11−13] self-cleaning,[5] and lubricity.[14−16] To accurately describe defect-containing networks, the main aim of this study is to use straightforward but accurate experiments and theoretical considerations to determine the structure−property relation of chemically cross-linked swollen polymer networks. Particular attention is dedicated to an accurate calculation of the molecular mass

between cross-links M_c from swelling experiments when the network contains dangling network chains, which can be seen as network defects.

Given the high importance of polyurethanes (PUs) in general,[1,17] and their potential use as hydrophilic networks in the biomedical field in particular, this study focuses on hydrophilic PU-networks. Because a well-defined network architecture is required, the use of an end-linking step growth polymerization chemistry is preferred over free radical initiated chain growth polymerization chemistries.[18,19] Poly(ethylene glycol) (PEG) is a hydrophilic polymer and is widely accepted in the biomedical field for its biocompatibility and antiprotein fouling properties.[4,16,20] Both PEG and PEG monomethyl ether (mPEG) are easily available in a range of well-defined molecular masses with low dispersity. Therefore, hydrophilic PU networks, built up of PEG, mPEG, and a tri-isocyanate cross-linker unit, were selected as model networks (see Figure 1).

In this study the preparation of PEG-based PU networks containing dangling mPEG network chains based on various PEG-diols, as well as mPEG concentrations and chain lengths, is described. The effect of the network precursor and dangling chain mass on the swelling properties of the formed networks was investigated experimentally. From a theoretical point of
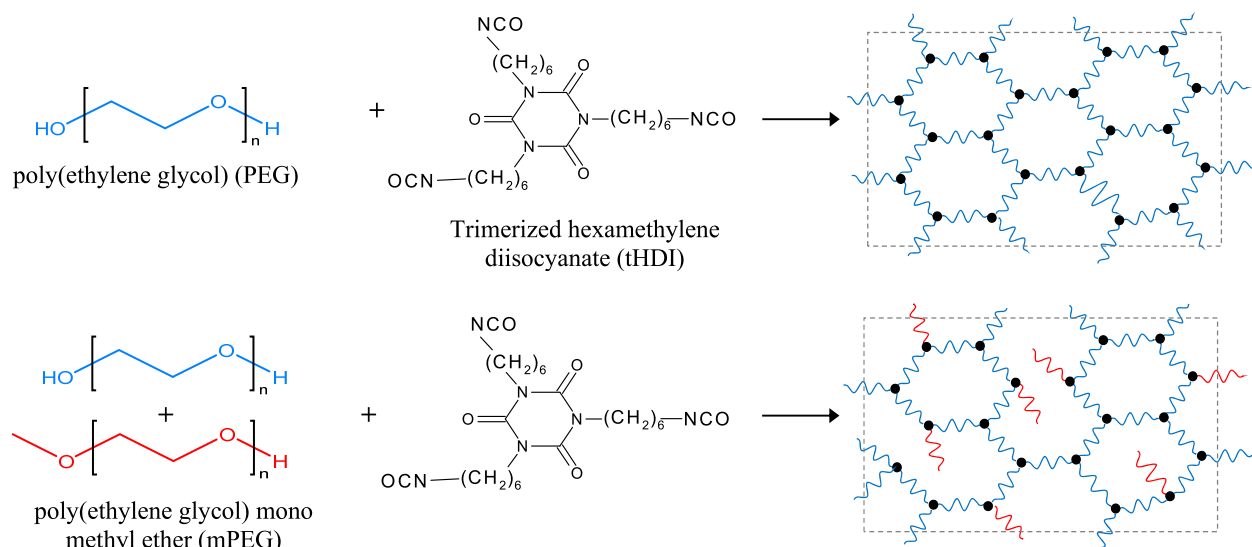
Figure 1. Schematic representation of selected model PEG-based PU network structures, without (top) and with (bottom) dangling network chains.

view, the use of the phantom network model for the description of the relation between the experimental swelling data and network structure is examined. For an accurate calculation of the molecular mass between cross-links of swollen PEG-based PU networks containing a high amount of dangling chains, fundamental corrections to the ideal network structure relations used in network models are proposed and validated. To that purpose network model essentials are briefly reviewed in the Supporting Information SI-I.

Polymeric Network Swelling. The affine or Flory–Rehner model[36−38] is widely used to calculate the cross-link density of polymer networks and is proven to be appropriate for networks with a low degree of swelling.[39] In the affine model the molecular mass between cross-links M_c is given by (see SI-I, eq SI-7 = eq 1)

$$M_c = -\frac{\rho_n V_s \varphi_{n_0}^{-1/3}\left(\varphi_n^{1/3} - \left(1 - \frac{2}{f}\right)\frac{\varphi_n}{\varphi_{n_0}}\right)}{\ln(1 - \varphi_n) + \varphi_n + \chi\varphi_n^2} \tag{1}$$

Here ρ_n is the density of the dry (nonswollen) network, V_s the molar volume of the solvent, φ_{n_0} the polymer volume fraction during the network formation (which is unity when the network is formed in the absence of solvent), f the functionality of the network junctions, φ_n the polymer network fraction in the swollen network, and χ the polymer–solvent interaction parameter.

The other model often used is the James–Guth phantom network model,[40,41] for which it is shown that it describes best the mechanical behavior of highly swollen polymer networks (including insights of NMR studies).[9,39,42−45] In this model M_c is given by (see SI-I, eq SI-8 = eq 2)

$$M_c = -\frac{\rho_n\left(1 - \frac{2}{f}\right)V_s\left(\frac{\varphi_n}{\varphi_{n_0}}\right)^{1/3}}{\ln(1 - \varphi_n) + \varphi_n + \chi\varphi_n^2} \tag{2}$$

However, real polymer networks contain physical chain entanglements[46−54] and network defects such as closed loops[55,56] and dangling chain ends.[57−62] These defects are hard to quantify while having a complex influence on the

mechanical properties of the network. A more recent approach[93,94] incorporated topological "loop" defects of various order in the classical phantom and affine network theories of elasticity. The results led to the so-called real elastic network theory (RENT) that describes how loop defects affect bulk elasticity, still in an approximate way. Hence, although both experimental and theoretical works have provided a better understanding of the influence of network imperfections on network swelling, theoretical descriptions of their effect on the network swelling are still largely absent. The only exception is a correction for dangling chain ends by Flory[24,63] in which the number of network chains is corrected to the number of elastically effective network chain elements ν_{eff} via $\nu_{eff} = \nu(1 - (2M_c/M_n))$ and using $\nu = V/(\rho_n^{-1}M_c)$, where M_n is the molar mass of polymer network chains before cross-linking and V the volume of the network. This correction is originally proposed for randomly cross-linked rubbers via vulcanization processes, in which tetrafunctional cross-links are formed by randomly joining two long chains.[24] Such a process inevitably leaves dangling chain ends in the network structure once no further reaction occurs further along the chain. From a fundamental point of view this correction is also suitable for random networks cross-linked by radiation[64] and is often used for hydrogel type networks in the biomedical field.[4,7] The correction is also applied for networks prepared from end-linking chemistries.[65−67] However, given the nature of the correction, its use for networks prepared from end-linking chemistries seems questionable.

Next to the expression for the dangling chains given by Flory, it should be noted that a great deal of work is done describing the effect of trapped chain entanglements inside the network. Half a century ago, Langley[46] introduced an expression for the so-called trapped entanglement factor T_e based on a probability approach, after which it became apparent that trapped entanglements significantly contribute to the elastic properties of polymer networks.[47,48,51] It is recognized that moduli from stress–strain experiments as well as the free energy terms from network models have to be properly corrected for the effect of entanglements. Although additional factors to take entanglements into account are

added to models, a comprehensive analytical description is absent.[9,10,35]

An interesting approach capable of estimating the effect of loops upon the shear modulus quantitatively is given by Zhong et al.[93] and Lang.[94,95] These authors showed that by quantifying the number of primary loops, the number of secondary and higher loops is fully fixed and that their effect can be fully incorporated in the description of network elasticity by using the concept of an effective phantom chain.

■ MATERIALS AND METHODS

Materials. Poly(ethylene glycol) (PEG) with different molar masses (M_n = 1000, 2000, 4000, 6000, 10000, and 20000 g mol^{-1}) and poly(ethylene glycol) monomethyl ether (mPEG) with different masses (M_n = 750, 2000, and 5000 g mol^{-1}, Sigma-Aldrich, all dispersities $Đ = M_w/M_n < 1.06$ (SEC)) were dried for 14 h at 40 °C at 20 mbar before use. Further purification of PEG via azeotropic distillation did not significantly improve the purity of the compounds, as shown by NMR. Trimerized hexamethylene diisocyanate (tHDI) (equivalent functional weight of 183 g mol^{-1} NCO (manufacturer value)) was kindly provided by Perstorp as tolonate HDT-LV2 and used as received. Cyclohexanone (99.8%, Sigma-Aldrich) was dried on molecular sieves before use.

Preparation of Polyurethane PEG-Diol-Based Networks. All glassware was dried in an oven at 100 °C at least 14 h prior to use. Network precursor stock solutions (typically 10 mL) of PEG (10−50 wt %) and of tHDI (50 wt %) were made by dissolving PEG and tHDI in cyclohexanone at 55 °C and room temperature, respectively. This was done in closed glass vials under an argon blanket and continuous stirring. Contact of oxygen with the network precursors was minimized as much as possible to prevent possible degradation of the polymers during network preparation. Therefore, every time a vial was opened during the whole preparation procedure, it was thoroughly flushed with argon after opening and before closure. Moreover, the lid was wrapped with Parafilm tape after closure.

Network formulation solutions (typically 10 mL) were prepared by mixing different ratios of precursor stock solutions in a closed glass vial at 55 °C under an argon blanket. The NCO/OH molar ratio of each formulation was kept at 1.1 to ensure full conversion of the OH groups and to compensate for possible side reactions. The formulation solutions were poured in precleaned and dried flat bottom aluminum foil molds with a diameter of 60 mm and put on a preheated heating element (65 °C) placed in a chamber (with a volume of ~1.5 dm³), which after closure was continuously flushed with dry N$_2$ (±150 L h^{-1} at 1 bar). The aimed thickness of the resulting dry films was controlled via the volume of the solution added to the molds.

The networks were formed by a solvent evaporation step of 2 h at 65 °C to remove both the solvent and oxygen present in formulation, followed by a final cure step of 1 h at 125 °C, both under a dry N$_2$ flow (±150 L h^{-1} at 1 bar). After curing, strips of 50 × 5 mm² were cut out with a standard laboratory razor blade and immersed in demineralized water to delaminate from the aluminum mold and to extract the extractable and/or unreacted components from the cured networks. Samples were dried at ambient conditions and subsequently for 14 h at 20 mbar at 40 °C and stored in a moisture-free desiccator after extraction. From here onward, purely PEG-diol-based PU networks will be named PUPEG (M_n of used PEG).

Networks containing mPEG dangling chains were prepared in a similar way as described above, with the exception that PEG/mPEG (10−50 wt %) network precursor stock solutions were used. Moreover, the weight ratios of the selected PEG and mPEG in each stock solution were chosen in such a way to yield similar molar OH$_{mPEG}$:NCO ratios, i.e., 1:9 or 1:30, for all PEG/mPEG networks to be comparable. From here onward, PEG-based PU networks containing mPEG dangling chains will be named PUPEG(M_n of used PEG)-mPEG(M_n of used mPEG) (OH$_{mPEG}$:NCO).

Experimental Network Formation Characterization. FTIR absorbance spectra of cured networks were recorded in attenuated total reflection (ATR) mode by using a Varian Excalibur FTIR-3100 equipped with a diamond Specac Golden Gate ATR setup. Measurements were performed over a spectral range of 4000 to 650 cm^{-1} with a resolution of 2 cm^{-1}. For each measurement 50 spectra were averaged. Next to recording the spectra of cured networks, the curing reaction at different temperatures of a PUPEG2000 network was followed in time on the ATR stage, equipped with an Eurotherm 2416 temperature controller. Approximately 10 mL of the network formulations was loaded on the ATR crystal, after which spectra were recorded every 30 s for a duration of 2 h under a continuous argon flow. For each measurement 12 spectra were averaged. Given the large overlap of the C=O urethane stretch vibration (1720 cm^{-1}) and the isocyanurate C=O stretch vibration (1675 cm^{-1}) present in the networks, and moreover the C−N urethane stretch vibration band (1550 cm^{-1}) being located at the fingerprint region, a reliable quantitative analysis of NCO to urethane conversion from the IR absorbance spectra is impracticable. Therefore, only the disappearance of the N=C=O asymmetric stretch vibration at 2270 cm^{-1} was used to analyze the NCO conversion of the cured networks at the surface. The normalization of the peak area was done by dividing its area by the peak area of the isocyanurate core vibration (766 cm^{-1})[68] and subsequently with this ratio between both peaks at t = 0 min.

The dry weight of the networks directly after curing and after extraction was measured gravimetrically. The amount of extractable material L gives a qualitative indication of the network formation and is calculated via $L = ((m_i − m_0)/m_i) \times 100\%$, where m_i and m_0 are the initial weight of a network after curing and of the extracted dry network, respectively. The extracted networks were immersed in demineralized water again to swell to equilibrium for at least 14 h. The swollen weight of the networks m_{eq} was measured gravimetrically directly after the networks were taken out of the water and after gentle removal of all excess water with absorbing lint free paper. Based on the absolute water uptake, the total polymer network volume fraction φ_n in the swollen network is calculated via

$$\varphi_n = \frac{V_n}{V} = \frac{V^0}{V} = \frac{1}{Q} \tag{3}$$

where V is the total volume of the swollen network, V_n is the volume of polymer network in the total swollen network, V^0 is the initial volume of the network before swelling, and Q is the volumetric equilibrium swelling ratio. Because the network is cross-linked in the absence of solvent (i.e., during the second step in the curing procedure), $V_n = V^0$. The swelling ratio Q can be calculated from the measured water uptake via

$$Q = \frac{V}{V^0} = 1 + \frac{\rho_n}{\rho_{H_2O}}\left(\frac{m_{eq}}{m_0} - 1\right) \tag{4}$$

where ρ_{H_2O} is the density of water (1 g cm^{-3}) and ρ_n the density of the nonswollen network. Values for ρ_n slightly differ for different network formulations, given the different overall network composition. Therefore, ρ_n of each different dry network is estimated via $\rho_n = \rho_{PEG}\varphi_{EG}^{vol} + \rho_{tHDI}(1 - \varphi_{EG}^{vol})$, assuming no excess volume upon mixing and polymerization, where ρ_{PEG} and ρ_{tHDI} are the densities of the PEG network precursors and tHDI in the network, respectively. Both are calculated with Molecular Modeling Pro software[69] using the molar volumes.[70] φ_{EG}^{vol} is the volume fraction of ethylene glycol (EG) units in the dry network and is calculated from the mass ratio of the network precursors via their densities by

$$\frac{1}{\varphi_{EG}^{vol}} = 1 + \frac{\rho_{PEG}}{\rho_{tHDI}}\left(\frac{1}{\varphi_{EG}} - 1\right) \tag{5}$$

where φ_{EG} is the initial weight fraction of EG units in the dry network. Finally, we note that preliminary attempts to characterize the films by mechanical measurement failed due to the extreme fragility of the films.

Table 1. Experimentally Measured Amount of Extractable Material L and Mass Ratio m_{eq}/m_0 and Theoretically Calculated Ethylene Glycol Fraction in Dry Network φ_{EG}, Dry Network Density ρ_n, and Polymer−Water Interaction Parameter χ Used To Calculate the Volumetric Swelling Ratio Q and the Polymer Fraction in Swollen Network φ_n of the Prepared PUPEG-Based Networks without MPEG Dangling Chains[a]

PUPEG	L [%]	m_{eq}/m_0 [g/g]	φ_{EG}	ρ_n [g cm^{-3}]	Q [V/V^0]	φ_n	χ
PEG1000	<0.1	2.22 ± 0.09	0.712	1.238	2.50 ± 0.11	0.400 ± 0.016	0.628 ± 0.008
PEG2000	<0.1	3.01 ± 0.17	0.835	1.222	3.45 ± 0.20	0.291 ± 0.017	0.582 ± 0.007
PEG4000	<0.1	3.81 ± 0.08	0.908	1.214	4.40 ± 0.10	0.227 ± 0.005	0.555 ± 0.002
PEG6000	<0.1	4.24 ± 0.19	0.937	1.210	4.92 ± 0.23	0.204 ± 0.009	0.546 ± 0.004
PEG10000	<0.1	4.58 ± 0.04	0.961	1.207	5.32 ± 0.05	0.188 ± 0.002	0.539 ± 0.001
PEG20000	<0.1	5.09 ± 0.12	0.980	1.205	5.93 ± 0.14	0.169 ± 0.004	0.531 ± 0.002

[a]Dry film thickness of all networks ± 120 μm. The error shows the mean absolute deviation from the mean value.

■ RESULTS AND DISCUSSION

Network Formation. It is critical to use a network preparation procedure that ensures proper network formation without leading to ambiguities in the structure analysis. This requires, first, the use of (nearly) monodisperse raw materials. Here raw materials with Đ = M_w/M_n < 1.06 were used for all components, so that in this study effects of polydispersity are minimal. As a second requirement, the degree of conversion should be (very near) unity. Therefore, the NCO conversion was followed in time, and the amount of extractable material after cross-linking was determined. Both led to the conclusion that (nearly) full conversion was reached. Hence, in this study fully cross-linked, monodisperse networks are employed.

After optimization, the two-step procedure, as described in the Materials and Methods section, was used for the preparation of the PUPEG2000 networks. The absence of the NCO asymmetric stretch vibration at 2270 cm^{-1} after cross-linking for 120 min at 125 °C in N$_2$ indicates a complete conversion of the NCO groups near the surface, while the increasing absorbance band at 1550 cm^{-1} shows the formation of urethane groups. Moreover, these films showed no curling during or after preparation was observed. No side reactions were observed, and the use of a N$_2$ atmosphere prevented the influence of water. Finally, hardly any extractable material was detected for these networks (Table 1). For a detailed analysis, see Supporting Information SI-II. An overview of the volumetric swelling ratio Q of PUPEG2000 networks prepared with varying film thicknesses (measured with a digital caliper with an accuracy of ±1 μm) and cast from network formulations with varying solid weight contents is also given in SI-II. No trends can be observed between the solid weight content of the network formulation, resulting film thickness, and volumetric swelling ratios of the networks, which indicates no influence of the film thickness on the swelling ratio of the networks prepared in this thickness range via the preparation procedure used.

Finally, it might be argued that the tHDI cross-linker, being a relatively hydrophobic molecule, associates in the (much) more hydrophilic environment of the coating components. In fact, this should than occur for all NCO ratios used. However, the amount of allophanates formed is proportional to the excess NCO, and no allophanates are observed for NCO:OH = 1.0 (as demonstrated by NMR, see SI-III). Furthermore, a close proximity of tHDI molecules is a prerequisite for allophanate formation (see SI-III). Finally, cross-linking is done at 125 °C so that association is typically small. Hence, we infer that any significant tHDI association during curing is highly unlikely.

PEG-Diol-Based PU Networks. PUPEG-based networks with a dry film thickness of ∼120 μm were used to study the experimental swelling properties for which at least six samples per network type were used. An overview of the measured amount of extractable material after curing L and mass ratio of networks swollen to equilibrium in water m_{eq}/m_0 is given in Table 1. The table also includes the theoretically calculated parameters for the ethylene glycol fraction in dry network φ_{EG}, network density ρ_n, and polymer−water Flory−Huggins interaction parameter χ used to calculate the volumetric swelling ratio Q and network volume fraction φ_n. Estimates for the values of χ for cross-linked networks are still a subject of debate, especially for hydrophilic networks and water.[34,45,71,72] Because of its dependence on the M_n of the precursors, φ_n of the networks, the actual chemical composition, and cross-link density,[73] the calculated values for χ of swollen cross-linked networks are always larger than those calculated from osmotic pressure data of linear polymers diluted in a solvent.[44,74−76] Therefore, caution is needed when using values for χ from the literature in the context of network swelling. Gnanou et al. obtained χ parameters for PUPEG-based networks[77] from swelling data in dioxane and water and elastic moduli arising from uniaxial compression measurements, ranging from 0.45 to 0.57 for polymer volume fractions between 0.033 and 0.259. By plotting their χ parameters versus the corresponding polymer volume fraction ρ_n for all available data, we obtained the following linear fit:

$$\chi = 0.46034 + 0.4195\varphi_n \tag{6}$$

Although the adjusted R^2 of the linear fit is only 0.64, nevertheless a linear fit still shows the best correlation. Given the close resemblance between their experimental networks and the networks studied in this work, the use of these experimentally determined χ parameters seems to be legitimate and the most accurate choice available.

The average amount of extractable material is less than 0.1 wt % for all network types and typically not measurable with the balance used (accuracy ±0.02 mg with a network weight in the range of 50−100 mg). This amount is lower than for most model studies reported so far. The calculated volumetric swelling ratio Q of the prepared PEG-diol based networks, shown as a function of the M_n of the PEG network precursor in Figure 2, clearly indicates a larger swelling ratio for networks prepared from precursors with a higher M_n, as expected upon decreasing the cross-link density of the network.

Corrections for Allophanate Formation for the Calculation of M_c. The absence of NCO peaks in the ATR-FTIR spectra indicates a complete disappearance of NCO groups in the network. For the network formation conditions used (T =
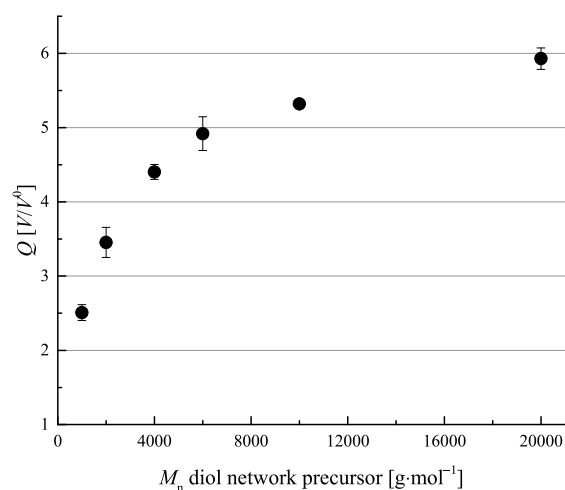
Figure 2. Mean volumetric swelling ratio Q of PEG-diol-based PU networks prepared with varying M_n of the diol network precursor and swollen to equilibrium in water. The error bars show the mean absolute deviation.

125 °C for 1 h) resulting in T_g on the order of -40 °C, allophanate formation[78−80] (reaction of an NCO group from a tHDI molecule with the N−H group of a urethane connected to another tHDI entity; see SI-III) has taken place, as proven by swollen state ^{13}C NMR. The formation of such allophanates gives rise to effectively five-functional cross-linking junctions, which, apart from the overall decrease of network junctions upon combination of junctions, will influence the swelling properties of the networks and needs to be taken into account when calculating the M_c. For the stoichiometric imbalance NCO:OH = 1.1, a small fraction of allophanates are formed. Moreover, for a ratio NCO:OH = 1.0, no allophanates are detected, while for a ratio 1.2 about twice the amount is observed as for 1.1 (see SI-III). Therefore, the excess of initial NCO groups is consumed via the formation of allophanates once no available OH groups are present anymore. Hence, 6 out of 11 three-functional tHDI molecules will combine into 3 five-functional network junctions (3 out of 33 NCO groups react with an already formed urethane given that NCO:OH = 1.1). From the initial 11 three-functional network junctions, 5 three-functional junctions still remain. Therefore, the overall network junction functionality f will become $(5{\cdot}3 + 3{\cdot}5)/8 = 3.75$, taking allophanate formation into account. As the amount of allophonate scales with the excess tHDI, $f = 3.75$ is used throughout. For further details, we refer to SI-III.

Network Swelling. As stated in the Introduction, the swelling behavior of the networks is expected to be best described by the phantom model. Furthermore, since the affine and phantom models are in fact the two limits of the more sophisticated Flory−Erman constrained junction model (see SI-I), the behavior of real swollen networks should indisputably lay between these limits. Calculated values for M_c from the measured swelling ratio for both the affine (eq 1) and phantom model (eq 2) for a 3-functional cross-linker, as well as the corrected phantom model taking into account the formation of allophanate by using $f = 3.75$, are given in Table 2 and shown in Figure 3a. All values used for the network parameters are given in Table 1, whereas the molar volume of water is taken as $V_s = 18.07$ cm^3. Figure 3 shows that two scaling regimes (for networks prepared with "high" and "low" M_n precursors) can be identified, regardless of the model used.

Table 2. Calculated Mean Mass between Cross-Links M_c of PEG-Diol-Based PU Networks Using the Affine Model (Eq 1), Phantom Model, and Phantom Model Corrected for Allophanate Formation (Eq 2)[a]

	mean M_c [g mol^{-1}]		
PUPEG	affine standard, $f = 3$	phantom standard, $f = 3$	phantom corrected, $f = 3.75$
PEG1000	1335 ± 213	542 ± 83	752 ± 119
PEG2000	3552 ± 562	1385 ± 210	1923 ± 308
PEG4000	6335 ± 318	2410 ± 116	3375 ± 162
PEG6000	7983 ± 752	3007 ± 271	4115 ± 306
PEG10000	9298 ± 174	3480 ± 62	4810 ± 137
PEG20000	11392 ± 509	4227 ± 181	5815 ± 164

[a]The error shows the mean absolute deviation from the mean value.

First, we focus on the low-M_n regime to elucidate on the validity of the different networks models, whereas in the next section the focus is put on a more detailed evaluation of the phantom model in which $f = 3.75$ is used. For networks prepared with low-M_n precursors (up to 4000 g mol^{-1}), the value for M_c calculated by using the affine model gives masses between cross-links on the order of 1.5 times higher than the M_n of the precursor used, while the phantom model yields masses on the order of 0.6 times the M_n of the precursors used. Assuming that the effect of trapped chain entanglements only plays a role in networks prepared from high-M_n precursors (see the next section), one expects a near one-to-one scaling of M_c with M_n for networks prepared with low-M_n precursors. The affine model yields a significantly higher M_c, which would indicate the formation of a loose network structure with a high fraction of network imperfections and unreacted precursors. Given the absence of extractable material after network formation (see Table 1), this scenario is highly contradicting, thereby confirming that this model is not describing the swollen networks properly.

On the other hand, the standard phantom model with $f = 3$ yields a M_c almost 2-fold lower than M_n. However, when an overall cross-link functionally of 3.75 is used in the phantom model, the slope of M_c vs M_n is near unity for the low-M_n precursors, as can be seen from Figure 3. This validates this corrected phantom model which takes the formation of allophanates into account. Next to the sensitivity of the model to the correct junction functionality, the model is extremely sensitive to the value for the polymer−water interaction parameter χ (see SI-IV). The chosen network polymer volume fraction dependent value for χ (eq 6), based on existing experimental data,[77] seems to be an accurate choice for describing these networks.

Network Swelling: The Effect of Trapped Physical Entanglements Using Precursors with $M_n > M_e$. A more detailed evaluation of the calculated M_c using the phantom model for which the junction functionality is corrected for allophanate formation is shown in Figure 3b. A clear transition of the slope of the curve is visible between networks produced with precursors with a M_n of 4000 and 6000 g mol^{-1}. Fitting the values of M_c of the networks prepared with $M_n \leq 4000$ g mol^{-1} to a weighted linear fit through the origin (Adj R^2 = 0.993) and the values of M_c of the networks prepared with $M_n \geq 6000$ g mol^{-1} to a weighted linear fit (Adj R^2 = 0.988) gives an intersect of both fits at a network precursor M_n of about 4500 g mol^{-1}. The slopes of both fits can be associated with all network junction constraints and network imperfections not
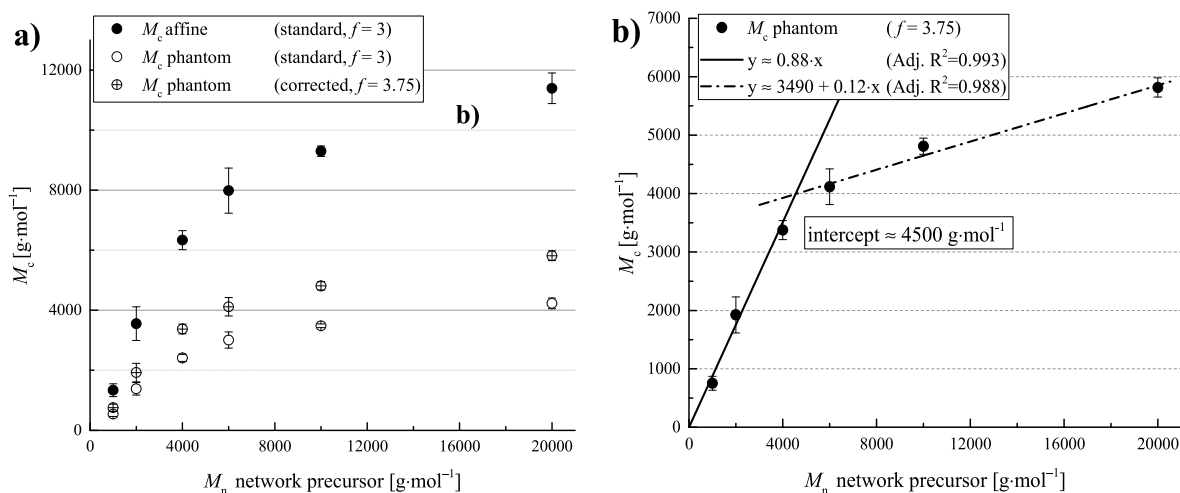
Figure 3. (a) Calculated mean mass between cross-links M_c of PEG-diol-based PU networks with varying network precursor M_n swollen to equilibrium in water. Calculated by using the affine model (solid, $f = 3$) (eq 1), the phantom model (open, $f = 3$) (eq 2), and corrected for allophanate formation (crossed, $f = 3.75$) (eq 2). (b) Calculated mean M_c by using the corrected phantom model for allophanate formation including two linear fit regimes. Solid line: weighted linear fit of the first 3 data points through the origin of the graph (Adj $R = 0.993$). Dotted line: weighted linear fit of last 3 data points graph (Adj $R^2 = 0.988$). The error bars show the mean absolute deviation.

accounted for in the theoretical network model. The transition from the first linear regime for M_c (for $M_n < 4500$ g mol^{-1}) to the second linear regime with a lower slope (for $M_n > 4500$ g mol^{-1}) can be seen as a transition between networks formed, both having a constant amount of topological constraints but with additional constraints for the second regime (more constraints → less network swelling → lower slope). From a molecular model point of view this can be interpreted as the additional contribution of trapped physical entanglements to the network modulus.[46−48] The M_n corresponding to the intersect (≈ 4500 g mol^{-1}) is apparently the molar mass of the network precursor above which trapped physical entanglements start to contribute to the network topology. This intersect value is close to the experimentally measured critical molar mass for PEG to form physical entanglements in the melt M_e (4410 g mol^{-1} for linear PEG)[81] as well as the calculated critical molar mass with the entanglement model proposed by Wool (4500 g mol^{-1}).[53] We conclude that near ideal networks are formed for PEG-diol-based PU networks using PEG with a M_n below M_e (given the slope of the fit 0.88), with a transition to PEG-diol-based PU networks which contain additional physical entanglements above this threshold.

Although it is known that trapped entanglements play an important role in the overall network properties, these studies often focused on randomly cross-linked networks and highly swollen gels with precursors (far) above M_e or ideal well-defined PDMS networks.[49,59,60,82−84] Less attention was given to describing the structure parameters based on swelling experiments of end-linked PEG networks or PU networks in general. It is argued by Lutz,[85] based on his data for one single PEG precursor with mass smaller than ≈ 4500 g mol^{-1} (namely 3000 g mol^{-1}), that the compressive modulus of PEG-based networks with that precursor M_n are lower as compared to networks with a higher M_n because of the absence of entanglements. Furthermore, Teodorescu et al.[86] based their choice of using PEG-based precursors with a M_n below 4400 g mol^{-1} to build cross-linked networks in view of the increased difficulties in interpretation of data when using precursors with a higher M_n. Hence, the clear relation between M_e of the PEG precursors and the changing slope of the M_c calculated from

swelling experiments as demonstrated here is, to the best knowledge of the authors, not reported in the literature so far for water swollen PEG-based PU networks.

PEG-Based PU Networks with MPEG Dangling Network Chains. Various PEG-based PU networks containing mPEG ($M_n = 750, 2000,$ and 5000 g mol^{-1}) were prepared to study the effect of the insertion of network dangling chains on the volumetric swelling ratio Q and the mass between cross-links M_c. These networks did not show either any NCO groups left after curing or the tendency to curl. Only the PUPEG1000mPEG5000 networks broke into smaller pieces during swelling and delamination of the mold, most likely due to too high swelling induced stresses in the network.

Proposed Corrections for the Calculation of M_c of PU Networks Containing Dangling Chains Defect. As stated before, except for the adjustments for randomly cross-linked linear long chains by Flory,[24] classical network models assume ideal network structure relations to calculate the mass between cross-links and/or network moduli. As shown by Saalwächter and co-workers[59,87] by ^{1}H double quantum low field NMR (DQ NMR) studies on PDMS networks, it is important to correct the phantom network model for the fraction of elastically active material in the network. For an estimate of the molar mass between cross-links M_c, they directly multiplied the numerator of eq 2 with the actual fraction of elastic active material as measured in their DQ NMR experiments.

Instead of proposing one single correction factor from experimental NMR data, we propose to use correction factors based on network structural arguments. A short dangling network chain is elastically inactive. Moreover, the moment a cross-linking point which is bearing a dangling chain has less than 3 connections to the "infinite" network, it is not an effective junction in the network anymore. Therefore, the presence of dangling chains in a network changes both ν and μ in the network structure relations (eq SI-3 to eq SI-5). Instead of using the ideal numbers for ν and μ, it would be more appropriate to correct both parameters for the effective amount of elastically active chains ν_{eff} and network junctions μ_{eff} via a simple correction factor

$$\nu_{\text{eff}} = \nu\alpha, \qquad \mu_{\text{eff}} = \mu\beta \tag{7}$$

$$\zeta = \nu_{\text{eff}} - \mu_{\text{eff}} + 1 \approx \nu_{\text{eff}} - \mu_{\text{eff}} \tag{8}$$

where α is the fraction of elastically active network chains in the network and β is the fraction of elastically active cross-link molecules (i.e., active network junctions). Equation 8 is proven to hold for networks of any functionality by Flory.[88] Substituting eq 7 into eq 8 and making again use of eq SI-11 modifies eq SI-5 to

$$\frac{\zeta}{V^0} = \frac{\left(\alpha - \left(\frac{2}{f}\right)\beta\right)\rho_n N_A}{M_c} \tag{9}$$

We propose to use eq 9 in combination with the expression for the elastic Helmholtz energy ΔA_{el} of a phantom network[9] as given by $\Delta A_{\text{el,ph}} = (\zeta kT/2)(\lambda_x^2 + \lambda_y^2 + \lambda_z^2 - 3)$ to yield the following corrected phantom model for the calculation of M_c for isotopically swollen PEG-based PU networks containing mPEG dangling network chains:

$$M_c = -\frac{\rho_n\left(\alpha - \left(\frac{2}{f}\right)\beta\right)V_s\left(\frac{\varphi_n}{\varphi_{n_0}}\right)^{1/3}}{\ln(1 - \varphi_n) + \varphi_n + \chi\varphi_n^2} \tag{10}$$

We estimate the values for α and β by making use of the Miller−Macosko−Vallés (MMV) statistical probability approach.[54,89−92] See SI-V for the derivations of the equations used for an $A_5A_3B_2B_1$ system. Such a system mimics network formation from two different types of A-bearing precursors ($f \geq 3$), a difunctional B-precursor, and a monofunctional B-precursor. Based on the network precursor ratio and the precursor parameters (f, M_n, and m), the average network structure can be calculated based on the overall extent of the reaction p via experimentally measured fraction of soluble material (extractable material) of the prepared networks. The MMV calculations yield estimated values for the weight fractions of the initial precursor material which end up as elastically active W_e, as inactive (i.e., pendant) W_p, or as soluble material W_s after network formation.

In this theoretical network structure formation an ideal network polymerization is assumed in which (1) all functional groups of the same type are equally reactive, (2) all functional groups react independently of each other, (3) there are no geometric restrictions for the precursors to find each other, and (4) no intramolecular reactions occur in finite species (no loop formation in soluble fraction). Moreover, next to the possibility for loop formation in real networks (and soluble material), no kinetic effects and topological restrictions on the possibility for the reactive groups to find each other after the gel point of the polymerization is reached are captured in the model. Neither are side-reactions and precursors with a deviating functionality (due to impurities, dispersity in initial components, or possible end-group degradation). Nevertheless, any deviation from the theoretical ideal network formation will increase the amount of network defects and thereby increase the amount of soluble material since it increases the chance that precursors are not connected to the infinite network structure. Note that it is possible that the actual soluble material consists of different individual structures which comprises one or more different network precursors. Therefore, by use of this approach, it is assumed that the measured amount of soluble material is a representative measure for the state of the average network

structure. Moreover, it is assumed that the experimental average final network structure can be related to the ideal theoretical average network structure at the calculated extent of the reaction based on the amount of measured soluble material.

If soluble material is detected after extraction, not all initial network precursors will end up being part of the network (i.e., soluble material will be washed away). Therefore, small corrections need to be applied to calculate the real effective fractions of the resulting extracted network (since this network will be the dry network which will be swollen during the swelling experiments). The fraction of elastically active material in the extracted network α is calculated by dividing W_e, obtained from the MMV calculation, by the fraction of material ending eventually ending up in the extracted network via

$$\alpha = \frac{W_e}{1 - W_s} \tag{11}$$

The same is true for the effective amount of elastically active network junctions in the network β. To take the allophanate formation into account, the system is corrected assuming that the initial 10% excess NCO leads to an instantaneous prereaction yielding a fraction of A_5 precursors before the cross-linking starts while the overall stoichiometric imbalance r is corrected to 1. The prereaction of 3 out of 33 NCO groups yields 3 5-functional cross-linkers while 5 3-functional cross-linkers remain (see SI-III). This results in a weight fraction of 5/11 for A_3 and 6/11 for A_5 of the initial cross-linker content.

A cross-linker molecule A_f or A_k will end up being an effective junction as long as it is connected with at least three ends to the infinite network structure. In other words, any cross-linker molecule that is connected with only two ends to the infinite network is still contributing to the weight fraction of elastically active material but is not an effective network junction anymore. Therefore, the actual mass between cross-links increases since the total mass of the elastic active components now is "shared" between less active cross-linking points. When the cross-linker molecule is only connected with one end to the infinite structure, it is neither elastically active nor an effective network junction. Therefore, the fractions of active cross-linker molecules $f_r A_{f,C}$ and $f_r A_{k,C}$ are given by

$$f_r A_{f,C} = \sum_{i=3}^{f} \left[\binom{f}{i} P(F_A^{\text{out}})^{f-i}(1 - P(F_A^{\text{out}}))^i \right] \tag{12}$$

$$f_r A_{k,C} = \sum_{i=3}^{k} \left[\binom{k}{i} P(F_A^{\text{out}})^{k-i}(1 - P(F_A^{\text{out}}))^i \right] \tag{13}$$

From these fractions, β is given by dividing the absolute weight fraction of active cross-linker molecules by those actually ending up in the network via

$$\beta = \frac{f_r A_{f,C} C_f + f_r A_{k,C}(1 - C_f)}{1 - (f_r A_{f,s} C_f + f_r A_{k,s}(1 - C_f))} \tag{14}$$

where $C_f = [A_f]/([A_f] + [A_k])$ is the ratio of the A-bearing precursors and $f_r A_{f,s}$ and $f_r A_{k,s}$ are the fractions of the cross-linker molecules ending up as soluble material.

Water Uptake and Amount of Extractable Material. An overview of the measured amount of extractable material L, volumetric swelling ratio Q, and PEG weight fraction φ_{EG} of all

Table 3. Amount of Experimentally Measured Extractable Material L, Calculated Theoretical Amount of Extractable Material L, Volumetric Swelling Ratio Q, and Ethylene Glycol Fraction of the Dry Networks φ_{EG} for PEG-PU Networks Containing mPEG Dangling Chains (NCO:OH = 1.1 for All Networks)[a]

PU network						
PEG	mPEG	OH_{mPEG}:NCO	exptl L [wt %]	ideal theor L [wt %]	Q [V/V^0]	φ_{EG}
1000	750	1:9	0.67 ± 0.52	0.086	2.70 ± 0.02	0.724
	2000	1:9	0.93 ± 0.07	0.165	3.21 ± <0.01	0.769
		1:30	0.38 ± 0.01	0.005	2.58 ± 0.01	0.732
	5000	1:9	b	0.291	4.42 ± 0.02	0.834
2000	750	1:9	0.32 ± 0.08	0.059	3.59 ± <0.01	0.829
		1:30	0.15 ± 0.04	0.001	3.33 ± 0.02	0.831
	2000	1:9	0.60 ± 0.33	0.117	3.97 ± 0.06	0.847
		1:30	0.56 ± 0.56[c]	0.003	3.40 ± 0.05	0.837
	5000	1:9	0.96 ± 0.96[c]	0.222	5.03 ± 0.03	0.878
		1:30	0.40 ± 0.36	0.007	3.84 ± <0.01	0.849
6000	750	1:9	0.39 ± 0.01	0.028	4.94 ± 0.03	0.933
	2000	1:9	0.67 ± 0.08	0.056	5.22 ± 0.01	0.935
		1:30	0.18 ± 0.18[c]	0.001	4.65 ± 0.01	0.937
	5000	1:9	0.60 ± 0.19	0.115	5.75 ± 0.04	0.941
10000	2000	1:9	0.93 ± 0.33	0.038	5.95 ± 0.03	0.959
		1:30	0.30 ± 0.13	0.001	5.55 ± 0.08	0.961
20000	750	1:9	0.55 ± 0.01	0.013	6.47 ± 0.02	0.978
	2000	1:9	0.83 ± 0.12	0.023	6.52 ± 0.02	0.978
		1:30	0.70 ± <0.01	0.0004	6.66 ± 0.14	0.980
	5000	1:9	3.25 ± 0.45	0.045	8.51 ± 0.16	0.979

[a]Dry film thickness of all networks ± 120 μm. Every sample was made twice. The error represents the mean absolute deviation from the mean value. [b]Unable to measure the amount of extractable material. [c]Amount of extractable material of one sample undetectable. Therefore, only data of the other sample was used.
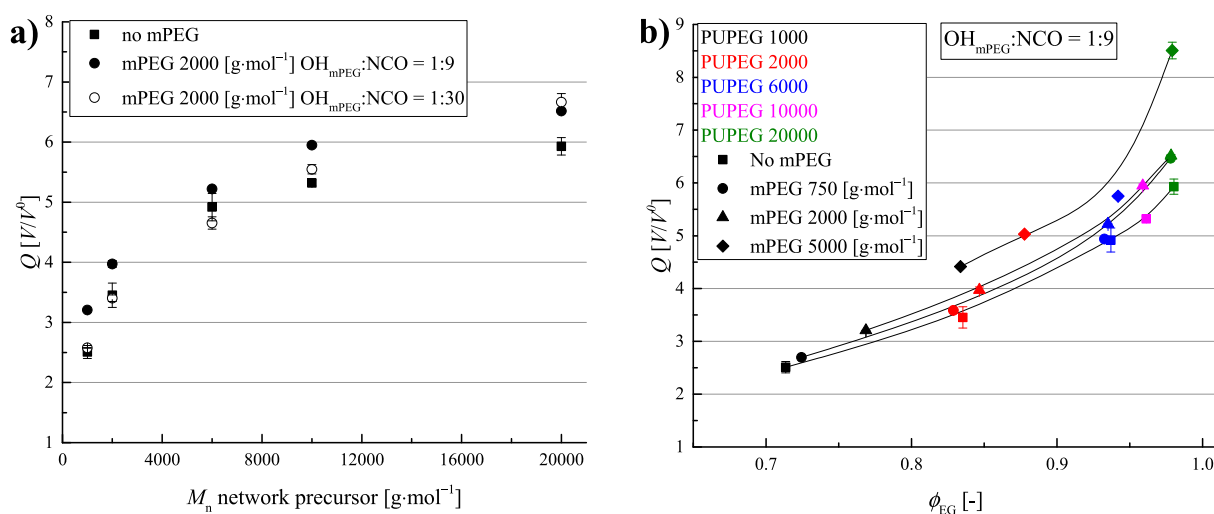

Figure 4. Mean volumetric swelling ratio Q of PEG-based PU networks with varying diol network precursor M_n swollen to equilibrium in water. (a) Plotted against M_n for networks without mPEG (squares) and with mPEG 2000 [g mol^{-1}] OH_{mPEG}:NCO = 1:9 (solid circles) or OH_{mPEG}:NCO = 1:30 (open circles). (b) Plotted against the total PEG fraction in the network φ_{EG} for networks with different M_n of the PEG-diol precursor (colors) and with or without mPEG of different molar mass (symbols) for networks with OH_{mPEG}:NCO = 1:9. Trend lines for networks with similar mPEG masses are shown to aid the eye. The error bars show the mean absolute deviation.

prepared PEG-mPEG based PU networks (all prepared in 2-fold) is given Table 3. The table also contains the theoretical values of extractable material as given by the calculated weight fraction of soluble material at the extent of the reaction for $p = 1$ for an $A_3A_5B_2B_1$ system, calculated by using the MMV probability approach. More details on the input parameters for the calculations are given in the next section. It can be seen from Table 3 that the networks prepared with mPEG precursors show a measurable fraction of extractable material,

in contrast to the mPEG free networks discussed previously. Moreover, the measured amount of extractable material is larger as expected from the calculated soluble fraction for ideal networks. This discrepancy indicates the presence of additional network defects since more material ends up in the soluble fraction after the network formation. A reason for this can be the fact that the probability approach does not consider topological restrictions on the functional groups (i.e., the physical possibility to meet each other at higher conversions)

Table 4. Overview of M_c Calculated by Using the Standard Phantom Model Taking into Account the Allophanate Formation (Eq 2), Calculated Fractions of Effective Elastically Active Material α (Eq 11), Calculated Effective Fraction of Active Network Junctions β (Eq 11), and M_c Calculated Using the Corrected Phantom Model Taking into Account the Allophanate Formation (Eq 10) for PEG-PU Networks Containing mPEG Dangling Chains (NCO:OH = 1.1 for All Networks)[a]

PU network				effective fraction corrections calculated using the MMV approach for a $A_3A_5B_1B_2$ system		
PEG	mPEG	OH_{mPEG}:NCO	mean M_c [g mol^{-1}] phantom f = 3.75	α	β	mean M_c [g mol^{-1}] phantom corrected, f = 3.75
1000	750	1:9	956 ± 25	0.79 ± 0.05	0.79 ± 0.06	760 ± 12
	2000	1:9	1597 ± 1	0.67 ± <0.01	0.79 ± <0.01	853 ± 2
		1:30	823 ± 7	0.84 ± <0.01	0.87 ± <0.01	659 ± 5
	5000	1:9	3418 ± 44	0.49[b]	0.82[b]	465 ± 6
2000	750	1:9	2127 ± 2	0.85 ± 0.01	0.80 ± 0.01	1946 ± 20
		1:30	1761 ± 39	0.91 ± 0.01	0.86 ± 0.01	1669 ± 50
	2000	1:9	2710 ± 110	0.77 ± 0.02	0.80 ± 0.03	1967 ± 41
		1:30	1861 ± 93	0.86 ± 0.08[c]	0.86 ± 0.09[c]	1624 ± 42
	5000	1:9	4422 ± 56	0.60 ± 0.01[c]	0.78 ± 0.02[c]	1766 ± 19
		1:30	2500 ± 5	0.83 ± 0.04	0.90 ± 0.05	1870 ± 47
6000	750	1:9	4241 ± 68	0.87 ± <0.01	0.77 ± <0.01	4216 ± 71
	2000	1:9	4715 ± 30	0.83 ± 0.01	0.76 ± 0.01	4274 ± 56
		1:30	3772 ± 201	0.86 ± <0.01[c]	0.82 ± <0.01[c]	3587 ± 18
	5000	1:9	5621 ± 78	0.78 ± 0.01	0.80 ± 0.02	4282 ± 11
10000	2000	1:9	5962 ± 64	0.82 ± 0.03	0.73 ± 0.03	5548 ± 79
		1:30	5262 ± 161	0.90 ± 0.02	0.85 ± 0.02	4991 ± 248
20000	750	1:9	6875 ± 47	0.86 ± <0.01	0.74 ± <0.01	6924 ± 39
	2000	1:9	6967 ± 46	0.83 ± 0.01	0.72 ± 0.01	6735 ± 112
		1:30	7240 ± 317	0.84 ± <0.01	0.79 ± <0.01	6613 ± 289
	5000	1:9	10805 ± 386	0.69 ± 0.01	0.61 ± 0.02	8916 ± 189

[a]Dry film thickness of all networks ± 120 μm. Every sample was made twice. Correction factors were obtained by using the MMV approach for a $A_5A_3B_2B_1$ system. The error represents the mean absolute deviation from the mean value. [b]Unable to measure the amount of extractable material. [c]Amount of extractable material of one sample was undetectable. Therefore, only data of the other sample was used.

nor takes possible loop formation or deviations in effective precursor functionality into account. Nevertheless, since the amount of extractable material for most networks is still less than 1 wt %, the networks are considered to be suitable for a reliable comparison of the absolute swelling ratios between them. Moreover, the measured amount of extractable material will be used in the next section to correct the theoretical network model for the presence of additional defects, as explained in the previous section.

Figure 4a shows the effect of introducing mPEG dangling chains (M_n = 2000 g mol^{-1}) on the volumetric swelling ratio Q of PEG-based PU networks with different M_n precursors. The respective networks without dangling chains are also shown for comparison. The figure shows that an addition of these mPEG dangling chains in a relative low amount of OH_{mPEG}:NCO = 1:30 to the network structure does not significantly change the water uptake for networks prepared from precursors with M_n < 10000 g mol^{-1}. However, upon increasing the mPEG content to OH_{mPEG}:NCO = 1:9, a clear increase in Q can be seen. These results indicate that for these networks only at high fractions of dangling chains a significant increase in water uptake can be expected, for which the relative contribution is largest for networks prepared from low-M_n PEG-diols.

Because tHDI is hydrophobic, the addition of mPEG dangling chains influences the overall fraction of hydrophilic material inside the networks. To see the actual network structural effect on the water uptake of these PEG-based PU networks, the networks are compared based on their overall ethylene glycol fraction φ_{EG} in Figure 4b (colors represent different PEG-diol M_n, whereas the symbols show the different

mPEG M_n, OH_{mPEG}:NCO = 1:9). Obviously, the addition of mPEG has the largest effect on φ_{EG} of PUPEG1000 networks (black). A comparison of the prepared networks based on their volumetric swelling ratio Q against φ_{EG} shows no crossing of the sketched trend lines between networks prepared with similar mPEG M_n and an increase in water uptake upon increasing M_n of mPEG, regardless of the PEG-diol precursor used. Furthermore, the graph shows the possibility to significantly increase the swelling ratio of PEG-based PU networks upon addition of dangling network chains, thus many opportunities for designing networks with similar (or different) Q having a different (or similar) φ_{EG}.

Corrections Due to the Presence of Network Defects for the Calculation of M_c. Next to the increase in overall water uptake, the addition of dangling chains to the network introduces network defects, as a dangling end can be seen as a defect itself. Moreover, the detection of extractable material after the network preparation indeed indicates the presence of additional defects since it exceeds the ideal theoretical amount of soluble material as shown in Table 3. These defects complicate an accurate calculation of M_c. Therefore, it is proposed to account for these defects by adapting the ideal network structure relation using effective fractions of elastically active material α and active cross-links β, calculated by using the MMV approach, as explained at the beginning of this section. Table 4 gives the calculated values for M_c obtained by using the phantom model with ideal structure relations (eq 2), correction factors α (eq 11) and β (eq 14), and the M_c from the corrected phantom model using these correction factors (eq 10) of the prepared PEG-mPEG-based PU networks.
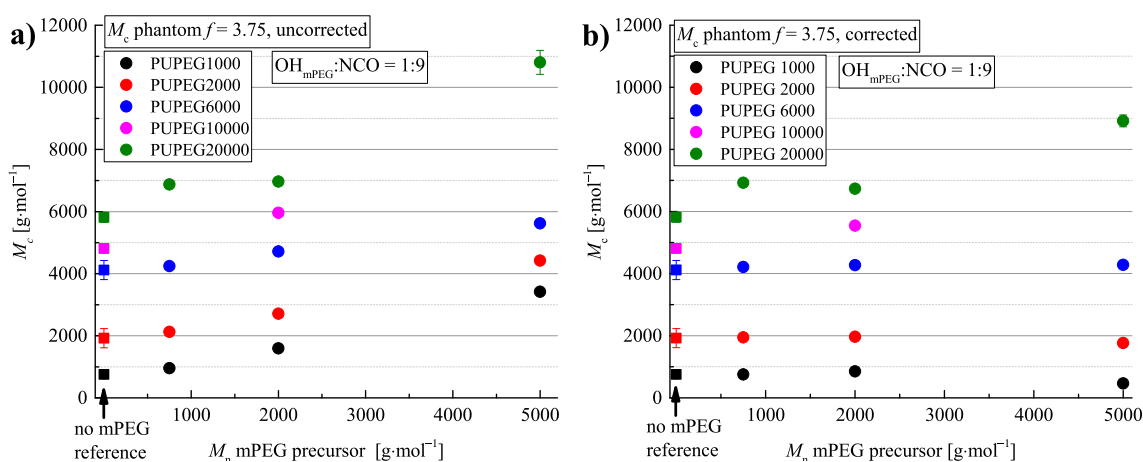
Figure 5. Calculated mean mass between cross-links M_c of PEG-mPEG PU networks with varying PEG-diol M_n swollen to equilibrium in water. Plotted against the M_n of the incorporated mPEG (OH_{mPEG}:NCO = 1:9) where the data points at 0 [g mol^{-1}] gives the M_c of the reference networks without mPEG. (a) Calculated by using the standard phantom model taking into account the allophanate formation (eq 2). (b) Calculated by using the corrected phantom model taking into account the allophanate formation (eq 10), corrected for effective elastically active fractions α and β, calculated by using the MMV approach for a $A_3A_5B_1B_2$ system. The error bars show the mean absolute deviation.

Again, the allophanate formation is taken into account in both models by using $f = 3.75$. The parameters α and β are calculated based on an $A_5A_3B_2B_1$ system and the experimentally determined fraction of extractable material as given in Table 3. The mass of an A_3 cross-linker molecule is taken as 549 g mol^{-1} (based on the actual manufacturer value of the tHDI used), whereas the mass of an A_5 cross-linker molecule is simply taken as twice the mass of an A_3 molecule in the calculations.

The M_c calculated by using the standard phantom model for all networks with a high amount of mPEG chains (OH_{mPEG}:NCO = 1:9) are shown versus the mPEG molar mass in Figure 5a. From a structural point of view, by keeping the amount of dangling chains constant, a significant change in M_c is not expected if only the length of the dangling chain is increased. This is particularly valid for networks of which both the PEG-diol and the mPEG chain are chosen with a M_n below the M_e of PEG, since this will not interfere with the formation (or removal) of physically trapped entanglements in the network. However, Figure 5a shows different trends for the M_c of the prepared networks when using the standard phantom model, given the observed mPEG M_n-dependent behavior. This shows that the standard phantom model is not able to predict an accurate M_c for these kinds of networks.

On the other hand, this behavior is observed for the M_c calculated from the corrected phantom model as can be seen in Figure 5b, in which a clear mPEG M_n independent behavior can be seen for the networks prepared with PEG-diol with $M_n \leq 6000$ g mol^{-1}. The calculated M_c for the PUPEG1000, -2000, and -6000 networks with mPEG chains of 750 and 2000 g mol^{-1} is slightly larger than the reference, as expected, since the presence of dangling chains reduces the amount of active cross-links when reacted with a 3-functional cross-linker (i.e., if a dangling chain reacts with an 3-functional cross-linker, the maximum amount of chains by which the cross-linker molecule is connected to the infinite network structure is less than 3 and therefore no longer an active cross-linking point). At the same time the total mass of the other two connected chains plus the mass of the cross-linker molecule itself is still elastically active material and thereby effectively increasing the overall M_c of the network. The slight decrease of apparent M_c for these networks

with an mPEG of 5000 g mol^{-1} is believed to be due to the formation of physical entanglements, since this precursor has a M_n above the M_e of PEG. The increase in M_c for PUPEG10000 and -20000 networks can be explained by exactly the opposite effect, since in these networks a fraction of the high-M_n PEG-diol is "replaced" by a low-M_n mPEG. Hereby, the amount of trapped physical entanglements is reduced, which leads to an overall higher value for M_c. Only the larger increase in the PEG20000-mPEG5000 networks seems to be overestimated. It should be noted that these networks showed a significantly higher amount of extracted material (3.25 wt %) (see Table 3) compared to all other networks (<1 wt %). Also, the fact that the swelling ratios of these networks were relatively higher provides confidence that this larger calculated M_c is real and due to more defects in these networks and not an error or limitation in the calculation method.

Finally, we need to address the effect of incomplete conversion, as treated by Lang et al.,[97] and the effect of loops, as has been recently treated by Zhong et al.[93] and Lang.[94] Incomplete polymerization leads to a lower value for the cycle rank per chain than the ideal $\zeta = 0.5$ for copolymerization, a typical estimate[96] for $f = 4$ being $\zeta = 0.314$ for a conversion of 0.875. From the fact that the amount of extractable material in our case is on average about 0.6%, we infer that the conversion is about 99.4%. This leads to a negligible effect of about 1% on the modulus. For the effect of loops the two treatments[93,94] essentially agree, although there are minor differences, which have been discussed by Lang.[95] The effect of loops is the largest for the smallest loops and the smallest molecular weight, i.e., for the PEG1000 system. Using the relevant data, the fraction of loops can be estimated[97] to be about 4%, leading to a decrease in modulus by a factor of about 0.96. For larger molecular weights this factor will be even closer to 1. Overall, these corrections are thus negligible.

Overall summarizing, we conclude that although the introduction of mPEG dangling chains introduces a change in polymer−solvent interaction, below the entanglement length the phantom network model describes the behavior well while clear reasons why above the entanglement length slight deviations occur have been elaborated in the discussion above.

CONCLUSIONS

The influence of the PEG-diol network precursor mass on the swelling ratio and network formation of hydrophilic PEG-based PU networks is studied, both experimentally and theoretically. Moreover, the study is extended to the influence of the presence of mPEG dangling network chains in the swollen networks. A suitable network preparation procedure is found to obtain networks that contain no residual NCO groups, amounts of extractable material below 1 wt %, and showed no tendency to curl.

The swelling behavior of PEG-based PU networks in water is best described by the phantom network, as expected. To calculate an accurate value for M_c of the prepared networks from the measured water uptake, allophanate formation, as shown to be present by swollen state ^{13}C NMR, needs to be taken into account when assigning the overall junction functionality of the networks (i.e., $f = 3.75$ in this work). Taking this into account the phantom model yields values for M_c which indicate a near-ideal network formation for low-M_n precursors (slope = 0.88), while the use of higher M_n precursors gives rise to the formation of trapped physical entanglements (slope = 0.12). The transition point from the near ideal regime to the entangled regime is found to coincide with the molar mass of PEG at which entanglements are formed in the melt (M_e). Although it is known that physical entanglements suppress the swelling of swollen polymer networks and increase their modulus, this is to the best knowledge of the authors the first time that this transition point is shown for swollen PU networks using a set of well-defined networks.

The addition of dangling chains to PEG-based PU networks will increase the swelling ratio of the networks, regardless of the PEG-diol precursor used. This allows some freedom in the design of hydrophilic networks with varying water uptake capabilities and network architectures. Furthermore, when comparing the swelling ratios of the mPEG containing networks with the actual content of hydrophilic material in the network, clear trends in swelling ratio for different dangling chain masses are found. Most notably, it is shown to be of utmost importance to correct for network imperfection when using standard network swelling models to calculate the M_c for these PEG-mPEG PU networks. This is essentially true for all polymeric networks prepared via end-linking polymerization reactions. The proposed corrections to the classical ideal network structure relations in combination with the statistical Miller–Macosko–Vallés approach to calculate overall network structure factors are shown to be able to predict an accurate value for the M_c of these swollen PEG-based PU networks containing high amounts of dangling network chains. This provides a new approach for studies which require an accurate estimate of M_c, only based on experimentally straightforward swelling experiments.

ASSOCIATED CONTENT

ⓈI Supporting Information

The Supporting Information is available free of charge at https://pubs.acs.org/doi/10.1021/acs.macromol.9b02275.

> Brief review of the theory of polymeric network swelling; influence film thickness and solid weight content formulation on the swelling ratio; discussion on allophanate formation; and influence χ on M_c and the

Miller–Macosko–Vallés recursive probability approach (PDF)

AUTHOR INFORMATION

Corresponding Authors

A. Catarina C. Esteves − *Laboratory of Physical Chemistry, Department of Chemical Engineering and Chemistry, Eindhoven University of Technology, Eindhoven, The Netherlands*; Email: a.c.c.esteves@tue.nl

Gijsbertus de With − *Laboratory of Physical Chemistry, Department of Chemical Engineering and Chemistry, Eindhoven University of Technology, Eindhoven, The Netherlands*; ⓞ orcid.org/0000-0002-7163-8429; Email: g.dewith@tue.nl

Authors

Peter T. M. Albers − *Laboratory of Physical Chemistry, Department of Chemical Engineering and Chemistry, Eindhoven University of Technology, Eindhoven, The Netherlands; Dutch Polymer Institute (DPI), 5600 AX Eindhoven, The Netherlands*

Leendert G. J. van der Ven − *Laboratory of Physical Chemistry, Department of Chemical Engineering and Chemistry, Eindhoven University of Technology, Eindhoven, The Netherlands*

Rolf A. T. M. van Benthem − *Laboratory of Physical Chemistry, Department of Chemical Engineering and Chemistry, Eindhoven University of Technology, Eindhoven, The Netherlands; DSM Ahead BV Netherlands, 6160 MD Geleen, The Netherlands*

Complete contact information is available at:
https://pubs.acs.org/10.1021/acs.macromol.9b02275

Notes

The authors declare no competing financial interest.

ACKNOWLEDGMENTS

REFERENCES

(1) Bhowmick, A. K.; Stephens, H. *Handbook of Elastomers*, 2nd ed.; Marcel Dekker, Inc.: 2001.

(2) Morton, M. *Rubber Technology*, 3rd ed.; Springer Science +Business Media, B.V.: 1999.

(3) Gyles, D. A.; Castro, L. D.; Silva, J. O. C.; Ribeiro-Costa, R. M. A review of the designs and prominent biomedical advances of natural and synthetic hydrogel formulations. *Eur. Polym. J.* **2017**, *88*, 373−392.

(4) Slaughter, B. V.; Khurshid, S. S.; Fisher, O. Z.; Khademhosseini, A.; Peppas, N. A. Hydrogels in regenerative medicine. *Adv. Mater.* **2009**, *21*, 3307−29.

(5) Esteves, A. C. C.; Lyakhova, K.; van der Ven, L. G. J.; van Benthem, R. A. T. M.; de With, G. Surface Segregation of Low Surface Energy Polymeric Dangling Chains in a Cross-Linked Polymer Network Investigated by a Combined Experimental-Simulation Approach. *Macromolecules* **2013**, *46*, 1993−2002.

(6) Zhang, Y.; Karasu, F.; Rocco, C.; van der Ven, L.; van Benthem, R. A. T. M.; Allonas, X.; Croutxe-Barghorn, C.; Esteves, A. C. C.; de With, G. PDMS-based self-replenishing coatings. *Polymer* **2016**, *107*, 249−262.

(7) Peppas, N. A.; Hilt, J. Z.; Khademhosseini, A.; Langer, R. Hydrogels in Biology and Medicine: From Molecular Principles to Bionanotechnology. *Adv. Mater.* **2006**, *18*, 1345−1360.

(8) Peppas, N. A.; Bures, P.; Leobandung, W.; Ichikawa, H. Hydrogels in pharmaceutical formulations. *Eur. J. Pharm. Biopharm.* **2000**, *50*, 27−46.

(9) Erman, B.; Mark, J. E. *Structure and Properties of Rubberlike Networks*; Oxford University Press, Inc.: 1997.

(10) Horkay, F.; McKenna, G. B. Polymer Networks and Gels. In *Physical Properties of Polymers Handbook*, 2nd ed.; Mark, J. E., Ed.; Springer Science + Business Media: New York, 2007; pp 497−523.

(11) Nurioglu, A. G.; Esteves, A. C. C.; de With, G. Non-toxic non-biocide-release antifouling coatings based on molecular structure design for marine applications. *J. Mater. Chem. B* **2015**, *3*, 6547−6570.

(12) Chen, S.; Li, L.; Zhao, C.; Zheng, J. Surface hydration: Principles and applications toward low-fouling/nonfouling biomaterials. *Polymer* **2010**, *51*, 5283−5293.

(13) Campoccia, D.; Montanaro, L.; Arciola, C. R. A review of the biomaterials technologies for infection-resistant surfaces. *Biomaterials* **2013**, *34*, 8533−54.

(14) Dunn, A. C.; Uruena, J. M.; Huo, Y. C.; Perry, S. S.; Angelini, T. E.; Sawyer, W. G. Lubricity of Surface Hydrogel Layers. *Tribol. Lett.* **2013**, *49*, 371−378.

(15) Gong, J. P. Friction and lubrication of hydrogels—its richness and complexity. *Soft Matter* **2006**, *2*, 544−552.

(16) Wyman, P. *Coatings for Biomedical Applications*; Woodhead Publishing Limited: 2012; Chapter 1.

(17) *Polyurethane Handbook: Chemistry, Raw Materials, Processing, Application, Properties*, 2nd ed.; Hanser Publishers: 1994.

(18) Rudin, A. *The elements of Polymer Science and Technology*, 1999.

(19) Hild, G. Model networks based on endlinking processes - synthesis structure and properties. *Prog. Polym. Sci.* **1998**, *23*, 1019−1149.

(20) Gullapalli, R. P.; Mazzitelli, C. L. Polyethylene glycols in oral and parenteral formulations-A critical review. *Int. J. Pharm.* **2015**, *496*, 219−239.

(21) Flory, P. J.; Rehner, J. Statistical Mechanics of Cross-Linked Polymer Networks II. Swelling. *J. Chem. Phys.* **1943**, *11*, 521−526.

(22) Rivlin, R. S. Large Elastic Deformations of Isotropic Materials 0.4. Further Developments of the General Theory. *Philos. Trans. R. Soc., A* **1948**, *241*, 379−397.

(23) Valanis, K. C.; Landel, R. F. Strain-Energy Function of a Hyperelastic Material in Terms of Extension Ratios. *J. Appl. Phys.* **1967**, *38*, 2997−3002.

(24) Flory, P. J. *Principles of Polymer Chemistry*; Cornell University Press: 1953.

(25) Flory, P. J.; Erman, B. Theory of elasticity of polymer networks 3. *Macromolecules* **1982**, *15*, 800−806.

(26) Ronca, G.; Allegra, G. Approach to Rubber Elasticity with Internal Constraints. *J. Chem. Phys.* **1975**, *63*, 4990−4997.

(27) Kloczkowski, A.; Mark, J. E.; Erman, B. A Diffused-Constraint Theory for the Elasticity of Amorphous Polymer Networks 0.1. Fundamentals and Stress-Strain Isotherms in Elongation. *Macromolecules* **1995**, *28*, 5089−5096.

(28) Edwards, S. F. Statistical Mechanics of Polymerized Material. *Proc. Phys. Soc., London* **1967**, *92*, 9−16.

(29) Edwards, S. F.; Vilgis, T. The Effect of Entanglements in Rubber Elasticity. *Polymer* **1986**, *27*, 483−492.

(30) Gaylord, R. J.; Douglas, J. F. The Localization Model of Rubber Elasticity. 2. *Polym. Bull.* **1990**, *23*, 529−533.

(31) Rubinstein, M.; Panyukov, S. Elasticity of polymer networks. *Macromolecules* **2002**, *35*, 6670−6686.

(32) Han, W. H.; Horka, F.; Mckenna, G. B. Mechanical and swelling behaviors of rubber: A comparison of some molecular models with experiment. *Math. Mech. Solids* **1999**, *4*, 139−167.

(33) Heinrich, G.; Straube, E.; Helmis, G. Rubber Elasticity of Polymer Networks - Theories. *Adv. Polym. Sci.* **1988**, *85*, 33−87.

(34) Quesada-Pérez, M.; Maroto-Centeno, J. A.; Forcada, J.; Hidalgo-Alvarez, R. Gel swelling theories: the classical formalism and recent approaches. *Soft Matter* **2011**, *7*, 10536.

(35) Treloar, L. R. G. *The Physics of Rubber Elasticity*, 3rd ed.; Clarendon Press: 1975.

(36) Flory, P. J.; Rehner, J. Effect of Deformation on the Swelling Capacity of Rubber. *J. Chem. Phys.* **1944**, *12*, 412−414.

(37) Kuhn, W. Dependence of the Average Transversal on the Longitudinal Dimensions of Statistical Coils Formed by Chain Molecules. *J. Polym. Sci.* **1946**, *1*, 380−388.

(38) Wall, F. T.; Flory, P. J. Statistical Thermodynamics of Rubber Elasticity. *J. Chem. Phys.* **1951**, *19*, 1435−1439.

(39) Erman, B.; Flory, P. J. Relationships between Stress Strain and Molecular Constitution of Polymer Networks - Comparison of Theory with Experiments. *Macromolecules* **1982**, *15*, 806−811.

(40) Guth, E.; James, H. M. Elastic and thermoelastic properties of rubberlike materials. *Ind. Eng. Chem.* **1941**, *33*, 624.

(41) James, H. M.; Guth, E. Theroy of rubber elasticity for development of synthetic rubbers. *Ind. Eng. Chem.* **1942**, *34*, 1365.

(42) Hild, G. Interpretation of equilibrium swelling data on model networks using affine and 'phantom' network models. *Polymer* **1997**, *38*, 3279−3293.

(43) Saalwächter, K.; Chassé, W.; Sommer, J.-U. Structure and swelling of polymer networks: insights from NMR. *Soft Matter* **2013**, *9*, 6587.

(44) Russ, T.; Brenn, R.; Geoghegan, M. Equilibrium swelling of polystyrene networks by linear polystyrene. *Macromolecules* **2003**, *36*, 127−141.

(45) Valentin, J. L.; Carretero-Gonzalez, J.; Mora-Barrantes, I.; Chasse, W.; Saalwachter, K. Uncertainties in the determination of cross-link density by equilibrium swelling experiments in natural rubber. *Macromolecules* **2008**, *41*, 4717−4729.

(46) Langley, N. R. Elastically effective strand density in polymer networks. *Macromolecules* **1968**, *1*, 348−352.

(47) Pearson, D. S.; Graessley, W. W. Structure of Rubber Networks with Multifunctional Junctions. *Macromolecules* **1978**, *11*, 528−533.

(48) Dossin, L. M.; Graessley, W. W. Rubber Elasticity of Well-Characterized Polybutadiene Networks. *Macromolecules* **1979**, *12*, 123−130.

(49) Sivasailam, K.; Cohen, C. Scaling behavior: Effect of precursor concentration and precursor molecular weight on the modulus and swelling of polymeric networks. *J. Rheol.* **2000**, *44*, 897−915.

(50) Schlogl, S.; Trutschel, M. L.; Chasse, W.; Riess, G.; Saalwachter, K. Entanglement Effects in Elastomers: Macroscopic vs Microscopic Properties. *Macromolecules* **2014**, *47*, 2759−2773.

(51) Kluppel, M. Trapped Entanglements in Polymer Networks and Their Influence on the Stress-Strain Behavior up to Large Extensions. *Phys. Polym. Networks* **1992**, *90*, 137−143.

(52) Acosta, R. H.; Monti, G. A.; Villar, M. A.; Valles, E. M.; Vega, D. A. Transiently Trapped Entanglements in Model Polymer Networks. *Macromolecules* **2009**, *42*, 4674−4680.

(53) Wool, R. P. Polymer entanglements. *Macromolecules* **1993**, *26*, 1564−1569.

(54) Campise, F.; Agudelo, D. C.; Acosta, R. H.; Villar, M. A.; Valles, E. M.; Monti, G. A.; Vega, D. A. Contribution of Entanglements to Polymer Network Elasticity. *Macromolecules* **2017**, *50*, 2964−2972.

(55) Lang, M.; Goritz, D.; Kreitmeier, S. Length of subchains and chain ends in cross-linked polymer networks. *Macromolecules* **2003**, *36*, 4646−4658.

(56) Vlasak, P.; Duskova-Smrckova, M.; Dusek, K. Structure development in polyurethane networks based on star-like precursors. *J. Coat. Techn. Res.* **2007**, *4*, 311−315.

(57) Andrady, A. L.; Llorente, M. A.; Sharaf, M. A.; Rahalkar, R. R.; Mark, J. E.; Sullivan, J. L.; Yu, C. U.; Falender, J. R. Model Networks of End-Linked Polydimethylsiloxane Chains 0.12. Dependence of Ultimate Properties on Dangling-Chain Irregularities. *J. Appl. Polym. Sci.* **1981**, *26*, 1829−1836.

(58) Patel, S. K.; Malone, S.; Cohen, C.; Gillmor, J. R.; Colby, R. H. Elastic-Modulus and Equilibrium Swelling of Poly(Dimethylsiloxane) Networks. *Macromolecules* **1992**, *25*, 5241–5251.

(59) Chasse, W.; Lang, M.; Sommer, J. U.; Saalwachter, K. Cross-Link Density Estimation of PDMS Networks with Precise Consideration of Networks Defects. *Macromolecules* **2012**, *45*, 899–912.

(60) Urayama, K.; Kawamura, T.; Kohjiya, S. Structure-mechanical property correlations of model siloxane elastomers with controlled network topology. *Polymer* **2009**, *50*, 347–356.

(61) Villar, M. A.; Valles, E. M. Influence of pendant chains on mechanical properties of model poly(dimethylsiloxane) networks 0.2. Viscoelastic properties. *Macromolecules* **1996**, *29*, 4081–4089.

(62) Bastide, J.; Picot, C.; Candau, S. Influence of Pendent Chains on the Thermodynamic and Viscoelastic Properties of Swollen Networks. *J. Polym. Sci., Polym. Phys. Ed.* **1979**, *17*, 1441–1456.

(63) Flory, P. J. Network structure and the elastic properties of vulcanized rubber. *Chem. Rev.* **1944**, *35*, 51–75.

(64) Peppas, N. A.; Merrill, E. W. Cross-linked PVA hydrogels swollen elastic networks. *J. Appl. Polym. Sci.* **1977**, *21*, 1763–1770.

(65) Zhu, C. C.; Bettinger, C. J. Photoreconfigurable Physically Cross-Linked Triblock Copolymer Hydrogels: Photodisintegration Kinetics and Structure-Property Relationships. *Macromolecules* **2015**, *48*, 1563–1572.

(66) Yang, T.; Long, H.; Malkoch, M.; Kristofer Gamstedt, E.; Berglund, L.; Hult, A. Characterization of well-defined poly(ethylene glycol) hydrogels prepared by thiol-ene chemistry. *J. Polym. Sci., Part A: Polym. Chem.* **2011**, *49*, 4044–4054.

(67) Rehmann, M. S.; Skeens, K. M.; Kharkar, P. M.; Ford, E. M.; Maverakis, E.; Lee, K. H.; Kloxin, A. M. Tuning and Predicting Mesh Size and Protein Release from Step Growth Hydrogels. *Biomacromolecules* **2017**, *18*, 3131–3142.

(68) Zhang, Y. A Spectroscopic study of the degradation of polyurethane coil coatings, PhD Thesis, Queen Mary, University of London, 2012.

(69) *Molecular Modelling Pro*, 6.3.3 ed.; Norgwyn Montgomery Software Inc., 1992.

(70) Van Krevelen, D. W. *Properties of Polymers*; Elsevier: 1990.

(71) Akalp, U.; Chu, S.; Skaalure, S. C.; Bryant, S. J.; Doostan, A.; Vernerey, F. J. Determination of the Polymer-Solvent Interaction Parameter for PEG Hydrogels in Water: Application of a Self Learning Algorithm. *Polymer* **2015**, *66*, 135–147.

(72) Horta, A.; Pastoriza, M. A. The interaction parameter of crosslinked networks and star polymers. *Eur. Polym. J.* **2005**, *41*, 2793–2802.

(73) Freed, K. F.; Pesci, A. I. Computation of the Cross-Link Dependence of the Effective Flory Interaction Parameter-Chi for Polymer Networks. *Macromolecules* **1989**, *22*, 4048–4050.

(74) Horkay, F.; McKenna, G. B.; Deschamps, P.; Geissler, E. Neutron scattering properties of randomly cross-linked polyisoprene gels. *Macromolecules* **2000**, *33*, 5215–5220.

(75) Horkay, F.; Burchard, W.; Hecht, A. M.; Geissler, E. Poly(Vinyl Alcohol Vinyl-Acetate) Copolymer Hydrogels - Scattering and Osmotic Observations. *Macromolecules* **1993**, *26*, 3375–3380.

(76) Eichinger, B. E.; Flory, P. J. Thermodynamics of Polymer Solutions 0.1. Natural Rubber and Benzene. *Trans. Faraday Soc.* **1968**, *64*, 2035.

(77) Gnanou, Y.; Hild, G.; Rempp, P. Molecular Structure and elastic behaviour of PEG networks swollen to equilibrium. *Macromolecules* **1987**, *20*, 1662–1671.

(78) Lapprand, A.; Boisson, F.; Delolme, F.; Méchin, F.; Pascault, J. P. Reactivity of isocyanates with urethanes: Conditions for allophanate formation. *Polym. Degrad. Stab.* **2005**, *90*, 363–373.

(79) Stern, T. Hierarchical fractal-structured allophanate-derived network formation in bulk polyurethane synthesis. *Polymers for Advanced Technologies*: 2017.

(80) Sekkar, V.; Gopalakrishnan, S.; Ambika Devi, K. Studies on allophanate–urethane networks based on hydroxyl terminated polybutadiene: effect of isocyanate type on the network characteristics. *Eur. Polym. J.* **2003**, *39*, 1281–1290.

(81) Aharoni, S. M. Correlations between Chain Parameters and the Plateau Modulus of Polymers. *Macromolecules* **1986**, *19*, 426–434.

(82) Obukhov, S. P.; Rubinstein, M.; Colby, R. H. Network Modulus and Superelasticity. *Macromolecules* **1994**, *27*, 3191–3198.

(83) Vega, D. A.; Villar, M. A.; Alessandrini, J. L.; Valles, E. M. Terminal relaxation of model poly(dimethylsiloxane) networks with pendant chains. *Macromolecules* **2001**, *34*, 4591–4596.

(84) Queslel, J. P.; Mark, J. E. Interpretation of the Moduli of Trifunctional Model Elastomers of Polydimethylsiloxane. *J. Polym. Sci., Polym. Phys. Ed.* **1984**, *22*, 1201–1210.

(85) Lutz, P. J. Structural properties of poly(ether) macromonomer based hydrogels. *Polym. Bull.* **2007**, *58*, 161–171.

(86) Teodorescu, M.; Cursaru, B.; Stanescu, P. O. Swelling and Diffusion Characteristics of Hydrogels Synthesized from Diepoxy-terminated Poly(ethylene glycol)s and Aliphatic Polyamines. *Soft Matter.* **2010**, *8*, 288–306.

(87) Chasse, W.; Lang, M.; Sommer, J. U.; Saalwachter, K. Cross-Link Density Estimation of PDMS Networks with Precise Consideration of Networks Defects (vol 45, pg 899, 2012). *Macromolecules* **2015**, *48*, 1267–1268.

(88) Flory, P. J. Elastic Activity of Imperfect Networks. *Macromolecules* **1982**, *15*, 99–100.

(89) Miller, D. R.; Macosko, C. W. New Derivation of Post Gel Properties of Network Polymers. *Macromolecules* **1976**, *9*, 206–211.

(90) Miller, D. R.; Valles, E. M.; Macosko, C. W. Calculation of Molecular-Parameters for Stepwise Polyfunctional Polymerization. *Polym. Eng. Sci.* **1979**, *19*, 272–283.

(91) Villar, M. A.; Bibbo, M. A.; Valles, E. M. Influence of pendant chains on mechanical properties of model poly(dimethylsiloxane) networks 0.1. Analysis of the molecular structure of the network. *Macromolecules* **1996**, *29*, 4072–4080.

(92) Bibbo, M. A.; Valles, E. M. Calculation of Average Properties of the Pendant Chains in a Network. *Macromolecules* **1982**, *15*, 1293–1300.

(93) Zhong, M.; Wang, R.; Kawamoto, K.; Olsen, B. D.; Johnson, J. A. Quantifying the impact of molecular defects on polymer network elasticity. *Science* **2016**, *353*, 1264–1268.

(94) Lang, M. On the elasticity of phantom model networks with cyclic defects. *ACS Macro Lett.* **2018**, *7*, 536–539.

(95) Lang, M. On the elasticity of polymer model neworks containing finite loops. *Macromolecules* **2019**, *52*, 6266–6273.

(96) Lang, M. Bildung und Struktur von polymeren Netzwerken, Dissertation. Ph.D. Thesis, Universität Regensburg, 2004.

(97) Lang, M.; Göritz, D.; Kreitmeier, S. Intramolecular Reactions in Randomly End-Linked Polymer Networks and Linear (Co)-polymerizations. *Macromolecules* **2005**, *38*, 2515–2523.